

**MASTER**

78-181

NOTE: This is a draft of a paper being submitted for publication. Contents of this paper should not be quoted nor referred to without permission of the authors.

[To be presented at the Laser-Solid Interactions and Laser Processing Symposium, Boston, Massachusetts, November 28-December 1, 1978]

## LASER ANNEALING OF ION IMPLANTED SILICON

C. W. White, J. Narayan and R. T. Young

By acceptance of this article, the publisher or recipient acknowledges the U.S. Government's right to retain a nonexclusive, royalty-free license in and to any copyright covering the article.

SOLID STATE DIVISION  
OAK RIDGE NATIONAL LABORATORY  
Operated by  
UNION CARBIDE CORPORATION  
for the  
U. S. DEPARTMENT OF ENERGY  
Oak Ridge, Tennessee

NOTICE  
This report was prepared as an account of work sponsored by the United States Government. Neither the United States nor the United States Department of Energy, nor any of their employees, nor any of their contractors, subcontractors, or their employees, makes any warranty, express or implied, or assumes any legal liability or responsibility for the accuracy, completeness or usefulness of any information, apparatus, product or process disclosed, or represents that its use would not infringe privately owned rights.

November 1978

DISTRIBUTION OF THIS DOCUMENT IS UNLIMITED

## **DISCLAIMER**

**This report was prepared as an account of work sponsored by an agency of the United States Government. Neither the United States Government nor any agency Thereof, nor any of their employees, makes any warranty, express or implied, or assumes any legal liability or responsibility for the accuracy, completeness, or usefulness of any information, apparatus, product, or process disclosed, or represents that its use would not infringe privately owned rights. Reference herein to any specific commercial product, process, or service by trade name, trademark, manufacturer, or otherwise does not necessarily constitute or imply its endorsement, recommendation, or favoring by the United States Government or any agency thereof. The views and opinions of authors expressed herein do not necessarily state or reflect those of the United States Government or any agency thereof.**

## **DISCLAIMER**

**Portions of this document may be illegible in electronic image products. Images are produced from the best available original document.**

THIS PAGE  
WAS INTENTIONALLY  
LEFT BLANK

## LASER ANNEALING OF ION IMPLANTED SILICON\*

C. W. White, J. Narayan, and R. T. Young  
Solid State Division, Oak Ridge National Laboratory  
Oak Ridge, TN 37830

### ABSTRACT

The physical and electrical properties of ion implanted silicon annealed with high powered ruby laser radiation are summarized. Results show that pulsed laser annealing can lead to a complete removal of extended defects in the implanted region accompanied by incorporation of dopants into lattice sites even when their concentration far exceeds the solid solubility limit. Implanted dopants are redistributed considerably by pulsed laser annealing, and parameters influencing the profiles are discussed. Calculations and experimental results provide strong evidence that the pulsed laser annealing mechanism involves melting of the crystal to a depth of several thousand angstroms, dopant diffusion in liquid silicon, and subsequent liquid phase epitaxial regrowth from the underlying substrate. The application of pulsed laser irradiation to materials processing areas other than ion implantation is briefly discussed.

### I. INTRODUCTION

Recent experiments have shown that high power pulses of laser radiation can be used successfully to anneal displacement damage in ion implanted semiconductors,<sup>1-4</sup> transform amorphous to single crystal layers,<sup>5</sup> dissolve precipitates in thermally diffused silicon,<sup>6,7</sup> and to form p-n junctions in silicon and gallium arsenide deposited with dopants.<sup>8</sup> In this paper we review the results of experiments carried out at the Oak Ridge National Laboratory (ORNL) to determine the physical and electrical properties of single crystal silicon implanted by B, P, As, Sb, Cu, and Fe and subsequently irradiated by high power radiation from a pulsed ruby laser. This work shows that pulsed laser annealing leads to a complete removal of displacement damage in the implanted region accompanied by the incorporation of the implanted dopants (B, P, As, Sb) into electrically active substitutional lattice sites even when the dopant concentration greatly exceeds the limit of solid solubility. In addition, implanted profiles are considerably changed by pulsed laser annealing due to the formation of a liquid layer several thousand angstroms thick during annealing, and subsequent dopant diffusion in the liquid state as discussed in a companion paper.<sup>9</sup> Profiles of implanted species after annealing are shown to depend on a number of factors, including laser energy density, number of successive pulses, extent of damage and/or dopant concentration, and segregation coefficient from the melt.

\* Research sponsored by the Division of Materials Sciences, U. S. Department of Energy under contract W-7405-eng-26 with the Union Carbide Corporation.

Finally, applications of pulsed laser irradiation to materials processing and fabrication not involving ion implantation are discussed.

## II. EXPERIMENTAL TECHNIQUES

Single crystal silicon wafers, (001) orientation, were used as substrates. Implants were carried out at room temperature under high vacuum conditions ( $2 \times 10^{-8}$  torr), at energies in the range 35 to 150 keV, and at doses in the range  $1 \times 10^{14}$  to  $1 \times 10^{17}/\text{cm}^2$ . Laser annealing was accomplished in air using the multimode output of a pulsed ruby laser with energy densities in the range 0.6 to 3.0  $\text{J}/\text{cm}^2$ , and pulse duration times in the range 20 to 60 nanoseconds (nsec). Following annealing, crystals were examined using transmission electron microscopy, Rutherford ion backscattering and ion channeling, and Van der Pauw measurements to determine the extent of remaining damage, the profile, and lattice location of the implanted species, and the electrical activity.

## III. ANNEALING OF LATTICE DAMAGE

Figure 1 shows transmission electron micrographs which compare directly the damage that remains in the lattice after laser annealing and conventional thermal annealing for silicon crystals implanted by B, P, As.<sup>1,2,10</sup> After thermal annealing at temperatures up to 1100°C, significant damage remains in the implanted region in the form of dislocation loops as shown in the right column of micrographs. By contrast, after laser annealing (~ 1.5  $\text{J}/\text{cm}^2$ , 60 nsec) no damage (dislocations, dislocation loops, or stacking faults) remains in the implanted region down to the resolution of the microscope (~ 10 Å). Diffraction patterns from these same crystals have no irregularities, and the orientation of the recrystallized region is the same as that of the underlying substrate, (001). Extensive experimental investigations<sup>7,11-14</sup> and theoretical calculations<sup>9,15,16</sup> provide strong evidence that pulsed laser irradiation under these conditions creates a melted region extending from the surface to a depth of several thousand angstroms. Recrystallization of the melted layer takes place by means of liquid phase epitaxial regrowth from the underlying substrate, resulting in defect free single crystal material with the same orientation as the substrate.

When the laser annealed crystals are subsequently heated to temperatures of 900°C to study the agglomeration of small defects, we observe only a very low number density ( $< 5 \times 10^{14}/\text{cm}^3$ ) of small defects (average diameter ~ 30 Å) in the implanted region. This shows that residual damage is very small after laser annealing. The conclusion from these experiments is that laser annealing is much more efficient in removing displacement damage than is conventional thermal annealing.

Figure 2 shows three different types of microstructure and crystal structure in the implanted region which was observed after annealing with different laser energy densities.<sup>3</sup> These results were

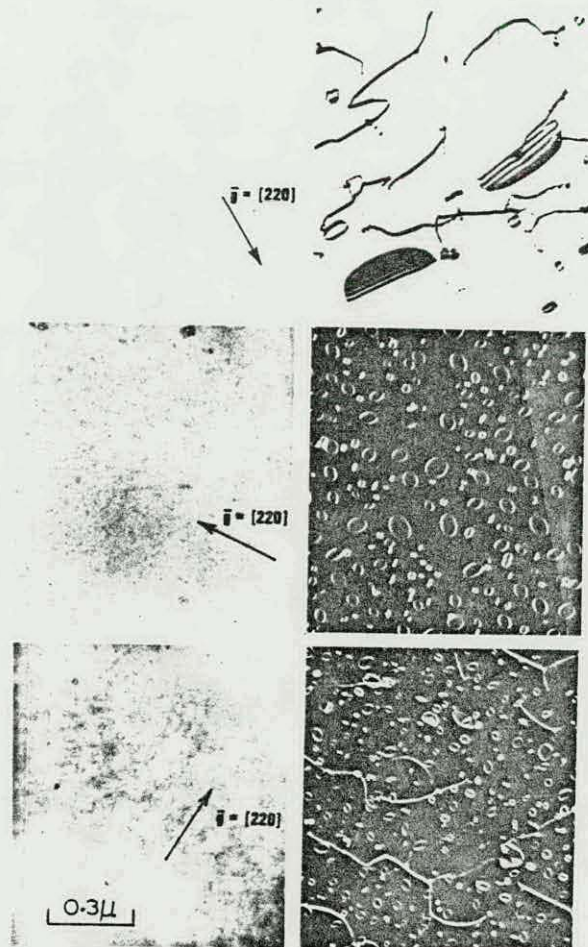


Fig. 1. Comparison of Laser (left column) and Thermal (right column) Annealing of Ion Implanted Silicon, (001) Orientation. Implanted Species, Energy and Dose were: Top Row -  $^{11}\text{B}$ (35 keV,  $3 \times 10^{15}/\text{cm}^2$ ); Middle Row -  $^{31}\text{P}$ (80 keV,  $1 \times 10^{15}/\text{cm}^2$ ); Bottom Row -  $^{75}\text{As}$ (100 keV,  $1 \times 10^{16}/\text{cm}^2$ ). Conditions for thermal annealing were  $\text{B}_2\text{P}(1100^\circ\text{C} - 30 \text{ mins})$ ;  $\text{As}(900^\circ\text{C} - 30 \text{ mins})$ . Conditions for laser annealing were  $1.5 \text{ J/cm}^2$ , 60 nsec.

obtained using silicon crystals implanted with  $^{75}\text{As}$ (100 keV,  $1.4 \times 10^{16}/\text{cm}^2$ ). Both ion channeling and transmission electron microscopy showed that a region  $\sim 1600 \text{ \AA}$  deep was made amorphous by implantation. Annealing with  $0.63 \text{ J/cm}^2$  caused a region  $\sim 1000 \text{ \AA}$  thick (determined by stereomicroscopy) to become polycrystalline as indicated by the diffraction pattern. This suggests that the crystal was melted to a depth of  $\sim 1000 \text{ \AA}$  and regrowth was not epitaxial because the melted region did not extend into the undamaged substrate. After annealing with  $1.07 \text{ J/cm}^2$ , which is very near the threshold for complete electrical activation, the electron diffraction pattern showed the recrystallized region to be single crystal indicating epitaxial regrowth, but a thin surface layer was observed containing residual damage in the form of dislocation loops. Stereomicroscopy showed the residual damage was confined to a depth of  $\sim 200 \text{ \AA}$ . The origin of this damaged layer at the surface is not well understood, but it may be related to solidification in the surface region due to radiant heat losses during the process of liquid phase epitaxial regrowth from the underlying substrate. Residual damage at the

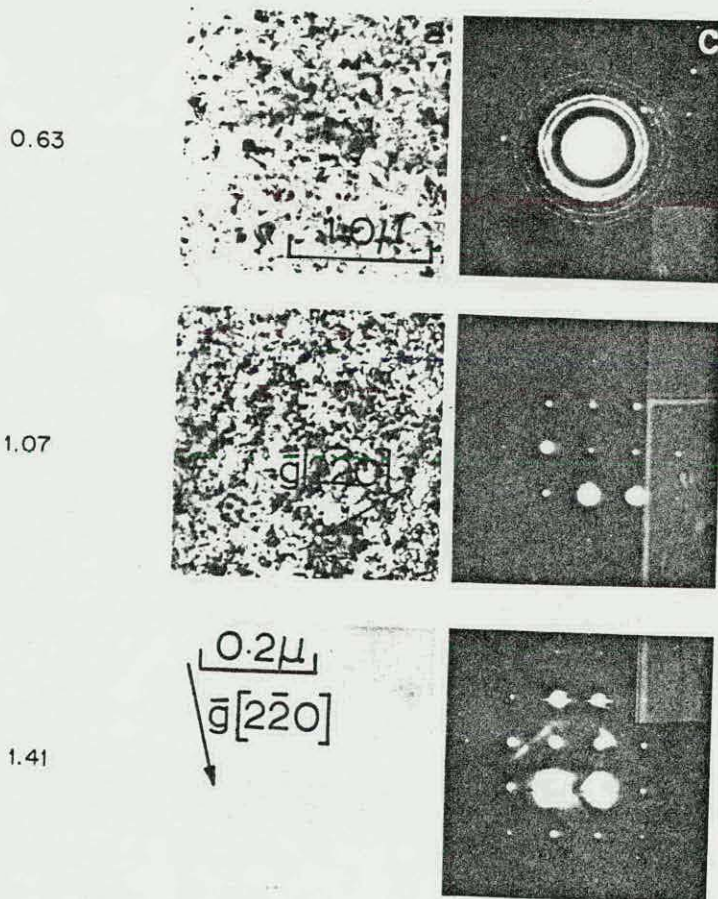
$^{75}\text{As}$  (100 keV,  $1.4 \times 10^{16} / \text{cm}^2$ )

Fig. 2. Microstructure Developed in Silicon by Annealing with Different Laser Energy Densities. The energy density used for annealing is indicated beside each micrograph and corresponding diffraction pattern. Pulse duration was 25 nsec.

surface has been observed for B, P and As implants after irradiation with laser energy densities very near the threshold for complete annealing ( $\sim 1.1 \text{ J/cm}^2$  for our implant conditions).<sup>28</sup> In Fig. 2, annealing with an energy density of  $1.4 \text{ J/cm}^2$  produced defect free single crystal material extending throughout the implanted region.

#### IV. EFFECT OF PULSED LASER ANNEALING ON DOPANT PROFILES

The effects of pulsed laser annealing ( $1.5 \text{ J/cm}^2$ , 60 nsec) on the profiles for implanted B, P, and As are shown in Fig. 3.<sup>11</sup> Profiles for B and P were measured by secondary ion mass spectrometry

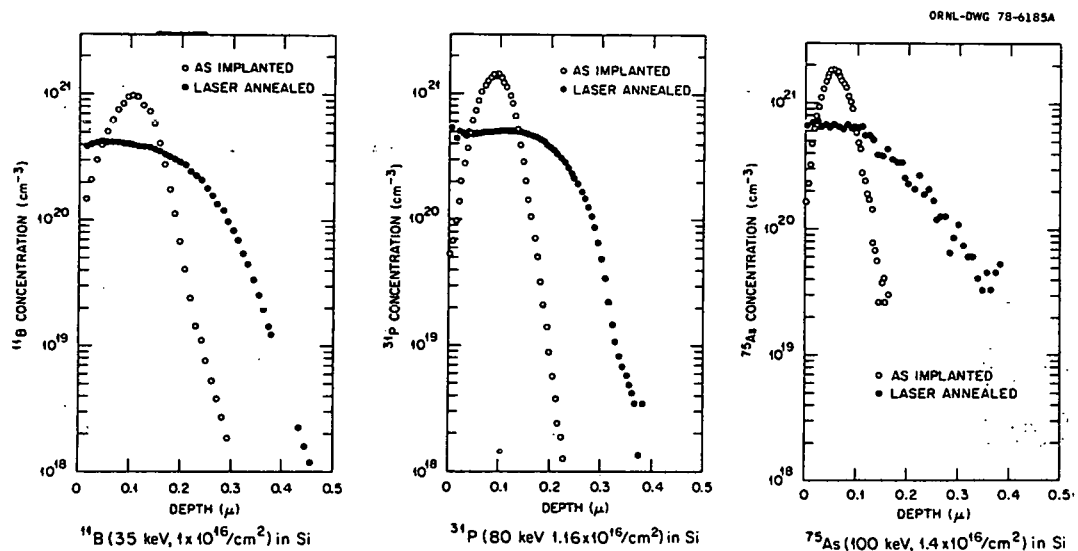


Fig. 3. Profiles of Implanted B, P, and As in Silicon

(SIMS) and those for As by 2.5 MeV He ion backscattering. In each case, the as-implanted profiles are very nearly Gaussian, but laser annealing causes a considerable redistribution of the implanted species both toward the surface and deeper into the crystal. Strong evidence has been presented to show that dopant redistribution takes place by diffusion in liquid silicon.<sup>9,15,16</sup> Calculations of the temperature distribution in the sample during and after the laser pulse show that the crystal can be melted to a depth of several thousand angstroms by the laser pulse. The melted region then recrystallizes from the underlying substrate by means of liquid phase epitaxial regrowth which takes place in a time of several hundred nanoseconds. During this time, implanted dopants can diffuse in the liquid where diffusion coefficients are orders of magnitude higher than in the solid.

Figure 4 shows a comparison of the As profile after laser annealing to a profile calculated assuming liquid phase diffusion. From the calculated profile, a value for the quantity  $(D\tau)$  is obtained, and the liquid phase diffusion time ( $\tau$ ) can be extracted from this by using a literature value<sup>17</sup> for the diffusion coefficient of As in liquid silicon. The result is  $\tau \sim 270$  nsec which is in reasonable agreement with published calculations of the thickness of the melted layers as a function of time.<sup>15,16</sup> Other examples of profile calculations are included in a companion paper.

Redistribution of dopants during laser annealing depends on the diffusion coefficient in the liquid and the time available for liquid phase diffusion. The profiles after laser annealing have been found to depend on a number of annealing parameters and material parameters including laser energy density, implant dose, number of successive

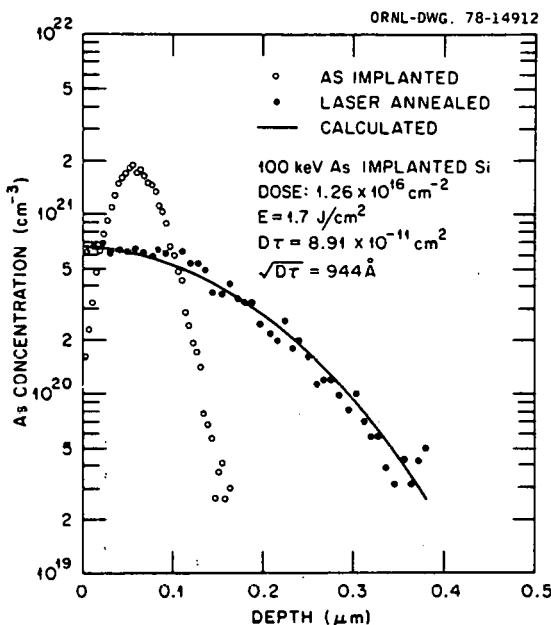


Fig. 4. Comparison of Profiles for Arsenic in Silicon with Calculations.

increased, redistribution of arsenic increases due to deeper penetration of the melt front and a correspondingly longer time available for diffusion in the liquid.

pulses, and the segregation coefficient from the liquid. Figure 5 shows the effect<sup>13</sup> of laser energy density on arsenic profiles in silicon crystals implanted by  $^{75}\text{As}$ (100 keV,  $1.4 \times 10^{16}/\text{cm}^2$ ). At the lowest laser energy density, arsenic is observed to be redistributed only in a depth interval extending from the surface to  $\sim 950 \text{ \AA}$ . The arsenic profile at greater depths after laser annealing is indistinguishable from that of the as-implanted crystal. This is interpreted to mean that at this laser energy density ( $0.63 \text{ J/cm}^2$ ) the melt front penetrated to  $\sim 950 \text{ \AA}$ , giving rise to arsenic redistribution in this region only. As the laser energy density is

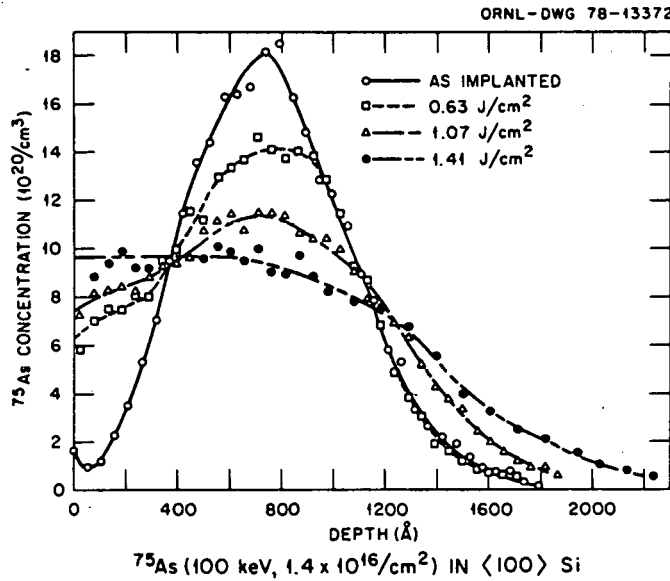


Fig. 5. Arsenic Profiles in Silicon after Annealing with Different Laser Energy Densities. Pulse duration time was 25 nsec.

Figure 6 shows boron profiles measured after laser annealing ( $1.6 \text{ J/cm}^2$ , 50 nsec) silicon crystals implanted to different boron

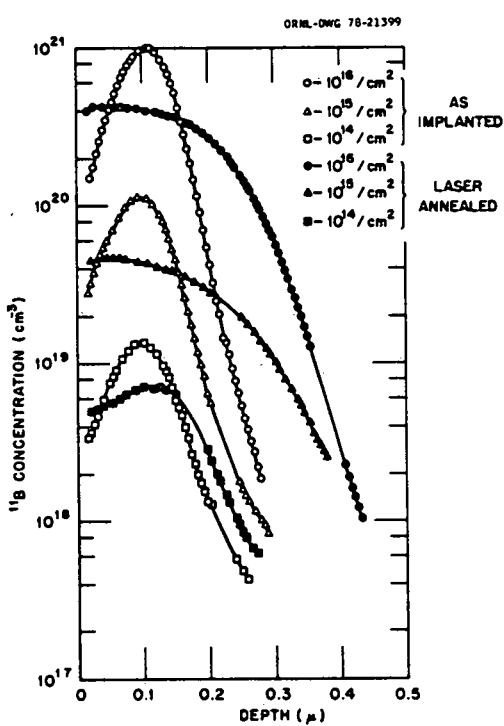


Fig. 6. Profiles of Boron Implanted to Different Doses in Silicon. The implant energy was 35 keV.

The final dopant profile also depends on the number of successive pulses. This is shown in Fig. 7 for the case of silicon crystals implanted by boron to doses of  $10^{15}$  and  $10^{16}/\text{cm}^2$  and annealed with one and two successive laser pulses ( $1.7 \text{ J/cm}^2$ , 50 nsec pulses). Most of the redistribution takes place during the first pulse, but additional redistribution is observed during the second pulse. These results show that the crystal can be remelted after the first laser pulse. This may occur due to increased free carrier absorption by the implanted dopant because calculations<sup>19</sup> show that for pure single crystal silicon the absorption coefficient is too low for melting to occur under these conditions.

The profiles after laser annealing for species with low segregation coefficients are radically different than for the case of B, P and As.<sup>13,20,21</sup> This is shown in Fig. 8 for the case of Cu and Fe in the as-implanted and laser annealed ( $1.4 \text{ J/cm}^2$ , 20 nsec) conditions. As indicated, laser annealing causes significant segregation of these species toward the surface. For copper, after laser annealing almost all of the impurity is localized to the first 200 Å of the surface region. The iron profile is distinctly shifted toward the surface. Segregation of these impurities toward the surface apparently is due to their very low segregation coefficients (defined as the ratio of concentrations in the solid and liquid phase,  $k = C_s/C_l$ ), which

doses in the range  $10^{14}$  to  $10^{16}/\text{cm}^2$ . The extent of boron redistribution and the shape of the final profile is almost the same for crystals implanted to  $10^{15}$  and  $10^{16}/\text{cm}^2$ , but is considerably less at a dose of  $10^{14}/\text{cm}^2$ . The increased redistribution at doses of  $10^{15}/\text{cm}^2$  and greater is believed related to more efficient absorption of laser light due to increased damage and/or dopant concentration in these crystals. The absorption coefficient at the Ruby wavelength is a strong function of the damage in the silicon crystals, being about an order of magnitude higher in amorphous silicon as compared to the single crystal case. In addition, the dopant concentration should increase the absorption coefficient due to free carrier absorption.<sup>18</sup> Increases in absorption coefficient lead to more efficient absorption of laser light, a longer melt duration time, and a correspondingly longer time for liquid phase diffusion.

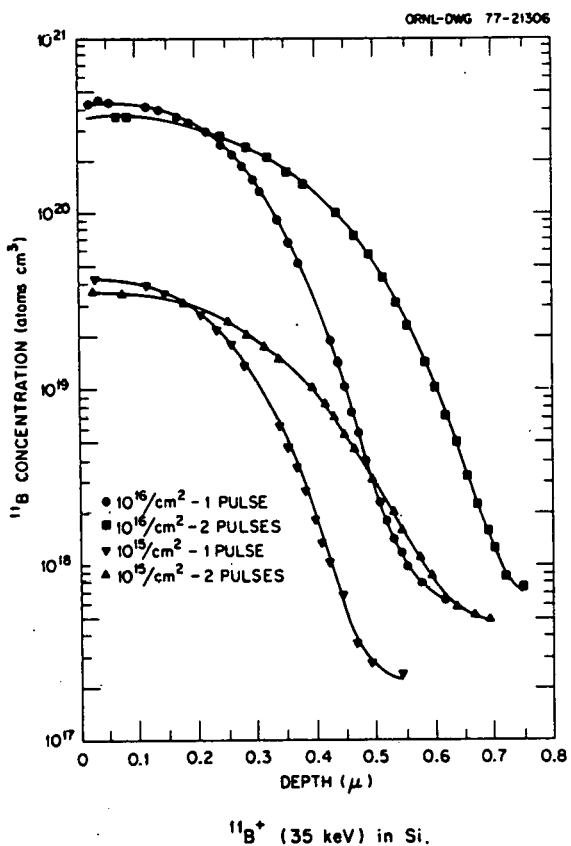


Fig. 7. Boron Profiles in Silicon after Annealing with Successive Laser Pulses. The implant energy was 35 keV.

are  $\ll 10^{-2}$ . In the process of liquid phase epitaxial regrowth, these species will be rejected into the liquid as the melt front approaches the surface. The enhanced concentration in the liquid is then transported toward the surface by the moving melt front and segregation occurs. The fact that Fe does not completely segregate to the surface during a single laser pulse may be related to a relatively low solubility and/or diffusion coefficient in liquid silicon. Further experiments are being carried out to clarify this. Comparison of the Fe profile results to calculations are presented in a companion paper.<sup>9</sup>

## V. LATTICE LOCATION AND ELECTRICAL PROPERTIES

Pulsed laser annealing is also capable of incorporating almost all of the implanted dopants (B, P, As and Sb) into electrically active substitutional lattice sites. Measurements of the lattice location of As and Sb have been made using 2.5 MeV He<sup>+</sup> ion back-scattering and channeling techniques.<sup>22-24</sup> Results for one of the crystals implanted by  $^{121}\text{Sb}$ (100 keV,  $1.6 \times 10^{16}/\text{cm}^2$ ) are summarized in Fig. 9. The aligned spectrum results (Fig. 9a) show that the crystal has been made completely amorphous by the implant to a depth of  $\sim 1400 \text{ \AA}$ . Laser annealing restores the single crystal order to the crystal because the aligned yield after annealing is very close

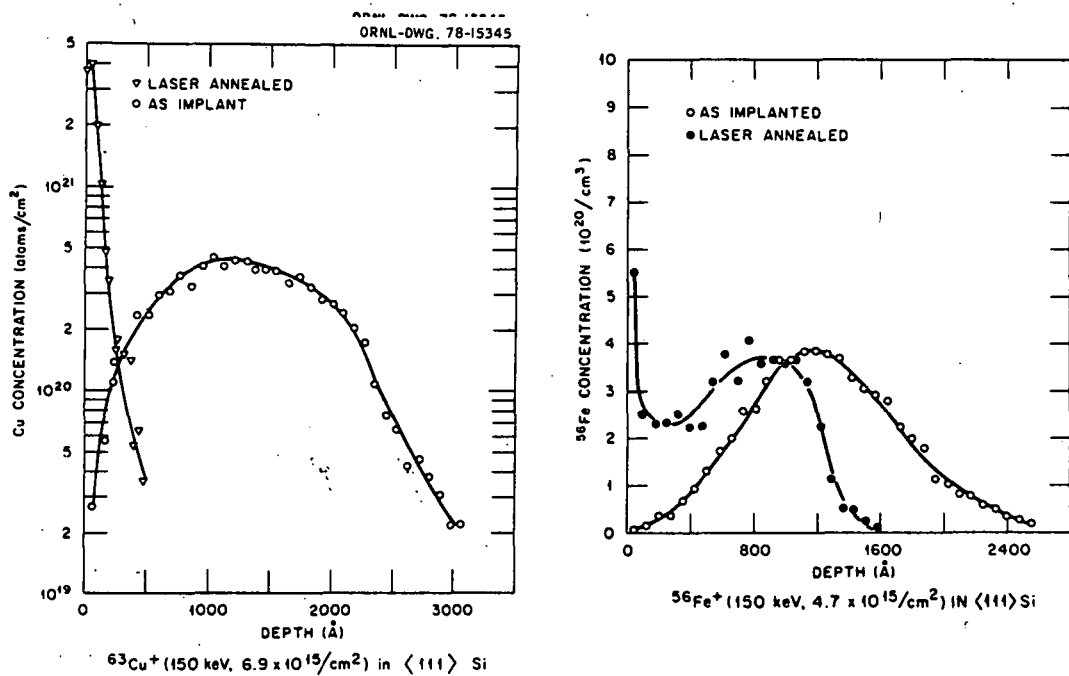


Fig. 8. Profiles for Cu and Fe in Silicon.

to that of the virgin crystal. The low yield of ions scattered from Sb after annealing shows that Sb is highly substitutional in the lattice. Fig. 9b shows detailed angular scans across two of the major axial directions. The yield curves of scattering from Sb and Si follow each other very closely, again showing that Sb is highly substitutional in the lattice. Quantitative analysis of this data shows that Sb is 98-99% substitutional in the lattice following laser annealing.

Figure 10 shows the measured electrical activity (obtained from Van der Pauw measurements) after laser annealing as a function of implanted dose for silicon crystals implanted with <sup>121</sup>Sb (100 keV). Lattice location measurements on these same crystals show that the Sb is 98-99% substitutional in the lattice for all crystals except the highest dose case, and Fig. 10 indicates that all the Sb is electrically active.<sup>22</sup> The electrical activity of the sample with the highest dose is slightly less than 100% due to precipitation of Sb in the very near surface region ( $\sim 300$  Å deep) during laser annealing, and a correspondingly lower substitutional fraction (87%).

Implanted arsenic has also been measured to be 98-99% substitutional in the lattice after laser annealing,<sup>22-24</sup> and electrical measurements show complete electrical activity.<sup>30</sup> In addition, boron<sup>1</sup> and phosphorous<sup>29</sup> show full recovery of electrical activity after laser annealing, although the carrier concentration of boron implanted crystals was measured to be somewhat higher than the implanted dose. The onset of full electrical activity correlates well with the threshold laser energy density required for complete removal of lattice damage.<sup>10,29</sup>

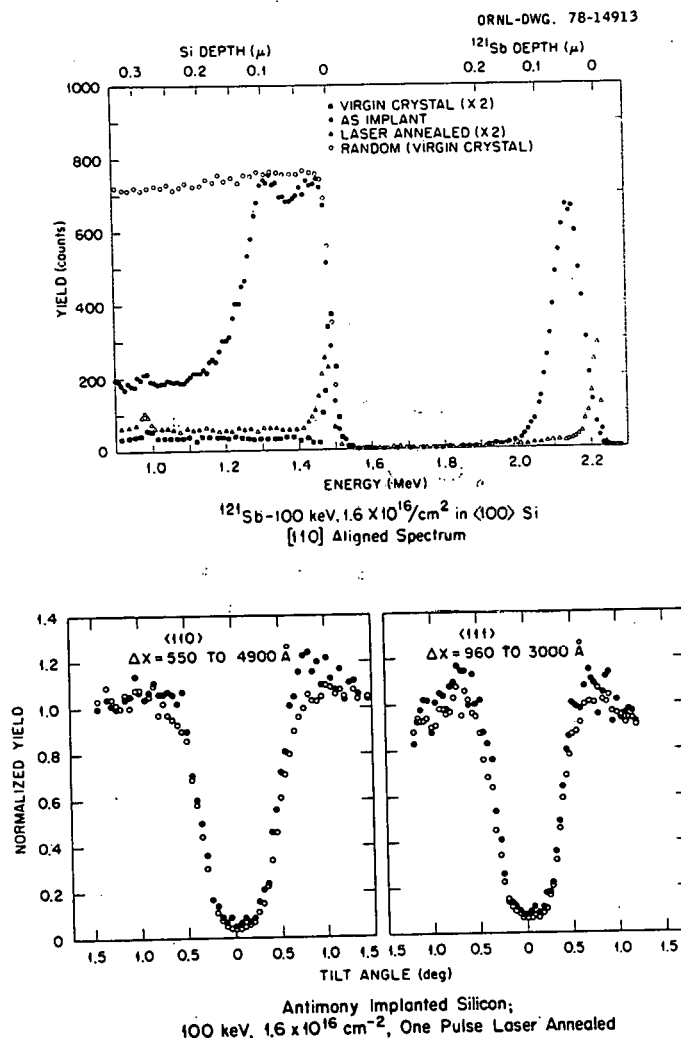


Fig. 9. (a) Aligned Spectrum Results for Sb Implanted Silicon. (b) Detailed Angular Scans Across [110] and [111] Directions. Open circles refer to scattering from Sb, closed circles refer to scattering from Si.

Incorporation of dopants such as Sb into electrically active substitutional lattice sites during pulsed laser annealing occurs even when the dopant concentration far exceeds the conventional limit of solid solubility. The Sb concentration in substitutional lattice sites for the crystals used in Fig. 10 extends up to  $1 \times 10^{21}/\text{cm}^3$  which is much greater than the limit of solid solubility ( $\sim 4 \times 10^{19}/\text{cm}^3$ ). Exceeding the limit of solid solubility by pulsed laser annealing apparently is related to the very short time associated with the annealing process. After the crystal is melted to a depth of several thousand angstroms by the laser light, liquid phase epitaxial regrowth takes place and dopants are incorporated into the solid at concentrations determined by the concentration in the liquid at the moving liquid-solid interface. Recrystallization takes place in a few hundred nanoseconds, and the recrystallized region then rapidly cools toward ambient temperatures in a few microseconds which is too short for the formation of precipitates in the solid phase.

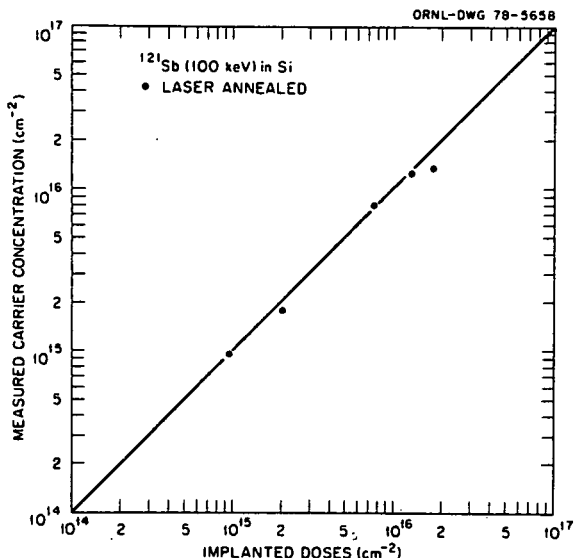


Fig. 10. Electrical Activity in Sb Implanted Silicon Crystals after Laser Annealing (1.7  $\text{J}/\text{cm}^2$ , 50 nsec).

Dopant concentration in excess of the solid solubility limit represents a supersaturated or metastable condition because precipitation of the excess dopant will occur if the laser annealed crystals subsequently are heated thermally.<sup>2</sup> This is shown in Fig. 11 for the case of silicon crystals implanted by a high dose of boron. Following laser annealing, the implanted region is defect free (left micrograph). Subsequent thermal heating to 900°C. for 30 mins causes precipitation of the excess boron as shown by the right micrograph. From the average size and number density of the precipitates, it is estimated that approximately 50% of the boron was contained in the precipitates. This agrees well with Van der Pauw measurements which showed a 50% decrease in the electrical activity after thermally heating the laser annealed crystal.

Several factors play a role in determining the maximum dopant concentration which can be incorporated into solid solution by pulsed laser annealing. One factor, which dominates in the case of boron, appears to be the contraction of the lattice in the implanted region.<sup>25,26</sup> Pulsed laser annealing can lead to a one dimensional contraction or expansion of the lattice in the implanted region. The sign of the lattice parameter change is determined by the size of the dopant atom (atomic radii) relative to silicon. The resulting strain in the contracted or expanded lattice is proportional to dopant concentration and when the strain exceeds the fracture strength of silicon, cracking will occur. Crystals implanted with boron to very high doses ( $\geq 5 \times 10^{16}/\text{cm}^2$ ) are observed to contain a high density of cracks,  $\sim 1\mu$  wide, in the implanted region after laser annealing. Presumably this occurs due to contraction of the lattice when boron atoms become substitutional during laser annealing.<sup>25</sup>

For the case of As and Sb, other factors limit the maximum obtainable concentration in solid solution. For very high dose implants of these species, precipitates are observed in the near

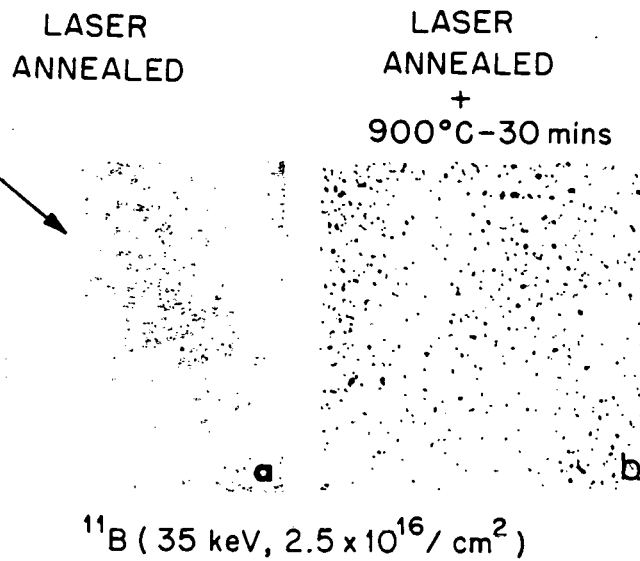


Fig. 11. Precipitation of Boron in Excess of Solid Solubility Limit. (a) After laser annealing; (b) laser annealed followed by thermal treatment.

surface region after laser annealing. Mechanisms responsible for the precipitation of these species have not been clearly determined, but this may be related to the dopant concentration exceeding the solubility limit in the liquid phase during epitaxial regrowth. Diffusion coefficients for these species in liquid silicon are large enough for precipitates or dopant rich regions to form in the liquid during recrystallization if the dopant concentration exceeds liquid phase solubility. Precipitates thus formed in the liquid would be incorporated into the solid during recrystallization. Diffusion coefficients are too small for these precipitates to be formed in the solid after recrystallization.

Recovery of electrical activity, removal of lattice damage, and incorporation of dopants into substitutional lattice sites is accomplished by pulsed laser annealing with no degradation of minority carrier lifetime in the substrate (for float-zone crystals). The excellent physical and electrical properties of laser annealed silicon are reflected in the performance of mesa diodes which have good diode parameters and low values of leakage current under reverse bias.<sup>29,30</sup> In addition, solar cells fabricated from boron implanted, laser annealed silicon have significantly improved quantum response and cell efficiency as compared to similar cells fabricated by thermal annealing.<sup>31</sup> These improvements are due to the better physical and electrical properties of laser annealed crystals.

## VI. APPLICATIONS TO OTHER MATERIALS PROCESSING AREAS

Melting produced by pulsed laser irradiation and rapid recrystallization of the melted region has very interesting possibilities in areas not directly involved with ion implantation. One application is the use of pulsed laser irradiation to dissolve precipitates in diffused materials.<sup>6,7,28</sup> This is demonstrated in Fig. 12a which shows boron profiles in the as-diffused and laser irradiated conditions for silicon crystals diffused with boron (1000°C - 10 mins). Diffusion of boron results in the formation of a layer ~ 200 Å thick with a very high concentration of boron atoms contained in the form of electrically inactive precipitates. Pulsed laser irradiation (1.5 J/cm<sup>2</sup>, 50 nsec) dissolves the precipitates as a result of melting and redistributes the boron as shown in Fig. 12a. Following irradiation no precipitates are present, the boron atoms are incorporated into substitutional lattice sites, and there is an order of magnitude increase in the electrically active carriers. Laser irradiation of these diffused crystals improves the p-n junction characteristics as determined from measurements on mesa diodes. Dissolution of precipitates in diffused crystals also provides a convenient technique to measure the depth of melting produced by pulsed laser irradiation.<sup>7,28</sup>

Another application involves the use of laser irradiation to form large area p-n junctions in silicon and GaAs by a process of

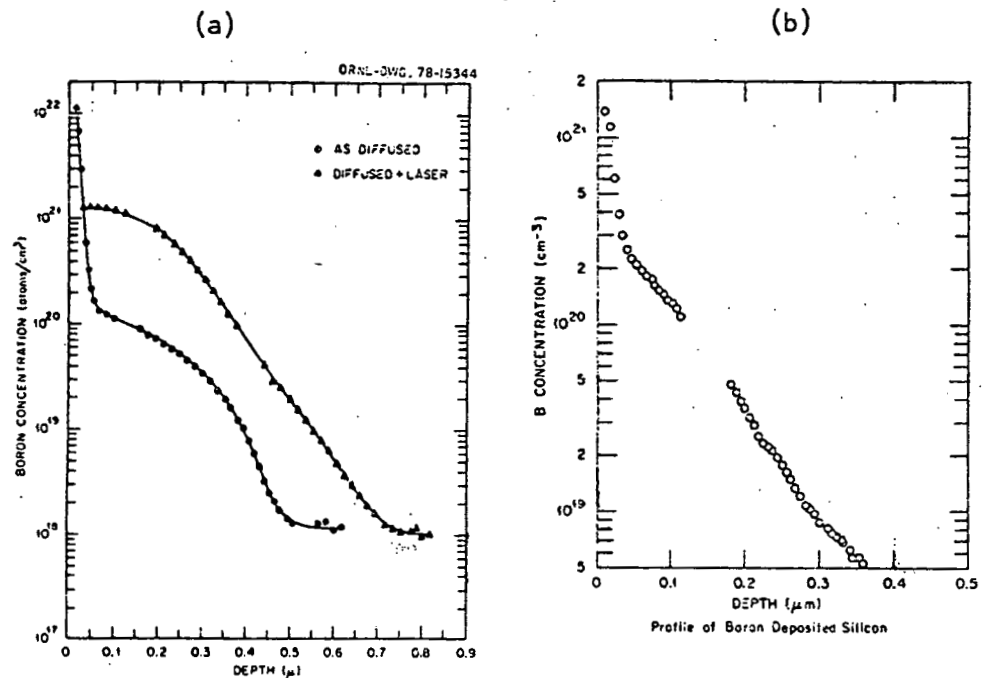


Fig. 12. (a) Boron Profiles in Boron Diffused Silicon.  
 (b) Profile of Boron in Silicon after Irradiation of a Crystal with Boron Deposited on the Surface.

laser induced diffusion.<sup>8,27</sup> For this application the dopant is first deposited on the surface as a film  $\sim 100 \text{ \AA}$  thick by evaporation. The deposited surface is then irradiated with pulsed laser light and during the time the near surface region is melted, the deposited dopant diffuses into the crystal and becomes electrically active. The profile of boron obtained after laser irradiation of boron deposited silicon is given in Fig. 12b and shows the penetration of boron to a depth of several thousand angstroms. This is a very attractive method for fabricating shallow p-n junctions because the depth of melting and subsequent dopant diffusion can be carefully controlled by the laser energy density.

## VII. CONCLUSIONS

Pulsed ruby laser annealing of ion implanted silicon can lead to complete removal of extended defects in the implanted region by the mechanism of liquid phase epitaxial regrowth. Complete annealing is accompanied by incorporation of dopants into electrically active substitutional lattice sites even when the dopant concentration greatly exceeds the conventional limit of solid solubility. Precipitation of dopant concentration in excess of solid solubility will occur if the laser annealed crystals are subsequently heated to temperatures of  $\sim 900^\circ\text{C}$ . Pulsed laser annealing leads to significant dopant redistribution and the final profiles have been shown to depend on laser energy density, number of successive pulses, segregation coefficient from the melt, and the extent of damage and/or dopant in the crystal. Comparison of calculations to experiments provides strong evidence that the pulsed laser annealing mechanism involves melting of the crystal by the laser light, diffusion of dopants in liquid silicon, and liquid phase epitaxial regrowth from the underlying substrate. In addition to ion implanted materials processing, pulsed laser irradiation is shown to have application as a means to dissolve precipitates in diffused crystals and as a method to introduce electrically active dopants into shallow regions by laser induced diffusion using crystals with dopants deposited on the surface.

## VIII. ACKNOWLEDGEMENTS

Work summarized here is the result of very close collaboration by many of our colleagues at ORNL. We wish to acknowledge the many important contributions by B. R. Appleton, W. H. Christie, G. J. Clark, B. C. Larson, P. P. Pronko, J. C. Wang, S. R. Wilson, R. F. Wood, and F. W. Young, Jr.

## IX. REFERENCES

1. R. T. Young, C. W. White, G. J. Clark, J. Narayan, W. H. Christie, M. Murakami, P. W. King, and S. D. Kramer, *Appl. Phys. Lett.* 32, 139 (1978). See particularly the cited references to pioneering work by Soviet scientists.

2. J. Narayan, R. T. Young, and C. W. White, *J. Appl. Phys.* 49, 3912 (1978).
3. J. Narayan, C. W. White, and R. T. Young, Proceedings of the International Conference on Ion Beam Modification of Materials, Budapest, Hungary, Sept. 4-8, 1978 (to be published).
4. G. K. Celler, J. M. Poate, and L. C. Kimmerling, *Appl. Phys. Lett.* 32, 464 (1978).
5. J. C. Bean, H. J. Leamy, J. M. Poate, G. A. Rozgonyi, T. T. Sheng, J. S. Williams, and G. K. Celler, *Appl. Phys. Lett.* 33, 227 (1978).
6. R. T. Young and J. Narayan, *Appl. Phys. Lett.* 33, 14 (1978).
7. J. Narayan, *Appl. Phys. Lett.* (in press).
8. J. Narayan, R. T. Young, R. F. Wood, and W. H. Christie, *Appl. Phys. Lett.* 33, 338 (1978).
9. J. C. Wang, R. F. Wood, C. W. White, B. R. Appleton, P. P. Pronko, S. R. Wilson, and W. H. Christie, these proceedings.
10. J. Narayan, R. T. Young, and C. W. White, p. 473 in Semiconductor Characterization Techniques, ed. by P. A. Barnes and G. A. Rozgonyi, The Electrochemical Society, New York, 1978.
11. C. W. White, W. H. Christie, B. R. Appleton, S. R. Wilson, P. P. Pronko, and C. W. Magee, *Appl. Phys. Lett.* 33, 662 (1978).
12. C. W. White, W. H. Christie, R. E. Eby, J. C. Wang, R. T. Young, and G. J. Clark, p. 481 in Semiconductor Characterization Techniques, ed. by P. A. Barnes and G. A. Rozgonyi, The Electrochemical Society, New York, 1978.
13. C. W. White, W. H. Christie, P. P. Pronko, B. R. Appleton, S. R. Wilson, R. T. Young, J. C. Wang, R. F. Wood, J. Narayan, and C. W. Magee, Proceedings of the International Conference on Ion Beam Modification of Materials, Budapest, Hungary, Sept. 4-8, 1978 (to be published).
14. D. H. Auston, C. M. Surko, T. W. C. Venkatesan, R. E. Slusher, and J. A. Golovchenko, *Appl. Phys. Lett.* 33, 437 (1978).
15. J. C. Wang, R. F. Wood, and P. P. Pronko, *Appl. Phys. Lett.* 33, 455 (1978).
16. P. Baeri, S. U. Campisano, G. Foti, and E. Rimini, *Appl. Phys. Lett.* 33, 137 (1978).
17. H. Kodera, *Japan J. Appl. Phys.* 2, 212 (1965).
18. A. A. Grinberg, R. F. Mekhtiev, S. M. Ryvkin, V. M. Salmanov, and I. D. Yaroshetskii, *Sov. Phys.-Solid State* 9, 1085 (1967).
19. R. F. Wood, private communication.
20. C. W. White, J. Narayan, B. R. Appleton, and S. R. Wilson, *J. Appl. Phys.* (January, 1979).
21. P. Baeri, S. U. Campisano, G. Foti, and E. Rimini, *Phys. Rev. Lett.* 41, 1245 (1978).
22. C. W. White, P. P. Pronko, S. R. Wilson, B. R. Appleton, J. Narayan, and R. T. Young, *J. Appl. Phys.* (February, 1979).
23. C. W. White, P. P. Pronko, B. R. Appleton, and S. R. Wilson, and J. Narayan, Proceedings of the International Conference on Ion Beam Modification of Materials, Budapest, Hungary, Sept. 4-8, 1978 (to be published).

24. S. R. Wilson, C. W. White, P. P. Pronko, B. R. Appleton, and R. T. Young, these proceedings.
25. B. C. Larson, C. W. White, and B. R. Appleton, *Appl. Phys. Lett.* 32, 801 (1978).
26. B. R. Appleton, C. W. White, B. C. Larson, J. Narayan, S. R. Wilson, and P. P. Pronko, these proceedings.
27. R. T. Young and J. Narayan, these proceedings.
28. J. Narayan and C. W. White, these proceedings.
29. R. T. Young, J. Narayan, C. W. White, R. F. Wood, J. W. Cleland, R. D. Westbrook, and P. M. Mooney, Proceedings of the International Conference of Ion Beam Modification of Materials, Budapest, Hungary, Sept. 4-8, 1978 (to be published).
30. R. T. Young, C. W. White, J. Narayan, G. J. Clark, and W. H. Christie, p. 466 in Semiconductor Characterization Techniques, ed. by P. A. Barnes and G. A. Rozgonyi, The Electrochemical Society, New York, 1978.
31. R. T. Young, J. Narayan, C. W. White, J. W. Cleland, W. H. Christie, and R. F. Wood, p. 1208 in Proceedings of the 13th IEEE Photovoltaic Specialists Conference - 1978, IEEE 78CH1319-3, New York, 1978.